

# Mechanisms of 5-Azacytidine-induced Toxicity and Repair System in the Developing Fetal Brain

胎仔中枢神経系における 5-Azacytidine による毒性発現  
および修復機構に関する研究

**Masaki Ueno**

Department of Veterinary Pathology  
Graduate School of Agricultural and Life Sciences  
The University of Tokyo

東京大学大学院農学生命科学研究科獣医病理学教室

上野 将紀

(平成14年度博士課程進学)

指導教官：土井 邦雄

# Contents

|   |     |
|---|-----|
| Introduction . . . . .  | 1   |
| Chapter 1 . . . . .   | 9   |
| 5-Azacytidine (5AzC)-induced Toxicity in the Developing Fetal Brain<br>: Cell Death and Cell Cycle Arrest |     |
| Chapter 2 . . . . .   | 41  |
| Molecular Mechanisms of 5-azacytidine (5AzC)-induced Toxicity<br>in the Developing Fetal Brain            |     |
| Chapter 3 . . . . .   | 71  |
| Repair Process after 5-Azacytidine (5AzC)-induced Injury<br>in the Developing Fetal Brain                 |     |
| Conclusions . . . . .   | 101 |
| References . . . . .  | 105 |
| Acknowledgements . . . . .  | 117 |

# Introduction

Environmental stresses and stimuli can induce deleterious effects on brain development. The fetal central nervous system (CNS) is sensitive to diverse environmental factors such as alcohol, heavy metals, irradiation, mycotoxins, neurotransmitters, and DNA damage, because a large number of processes occur during an extended period of development and fetal neural damage is an important issue affecting the completion of normal CNS development (Fig. I-1; Rodier, 1995; Mendola et al., 2000; Costa et al., 2004).

In the developing brain, multipotent neural progenitor cells proliferate in the ventricular zone (VZ), and then they differentiate into neurons and, later, glial cells (astrocytes and oligodendrocytes) (Rao, 1999; Qian et al., 2000; Temple, 2001). They form a pseudostratified epithelium in the VZ in the early developmental stage, where they are called neuroepithelial cells, and later, they project their fibers from the ventricular surface to the pial surface, where they are called radial glia. The nuclei of proliferating neural progenitor cells undergo a characteristic migration—interkinetic nuclear migration (or “elevator movement”) —in the VZ, in which the positions of nuclei are correlated with their cell cycle phase (Sauer and Walker, 1959; Fujita, 1960, 1962, 1963, 2003; Yoshida et al., 1987; Takahashi et al., 1992, 1993) (Fig. I-2). S phase nuclei, located in the outer area of the VZ, migrate inward during G2 phase, and mitosis occurs at the ventricular surface. The nuclei then migrate outward during G1 phase and enter S phase again. In this way, neural progenitor cells proliferate. After mitosis, some of them migrate beyond the VZ, where they differentiate into neurons or glial cells to form the neural network, e.g. cortex in the telencephalon (Fig., I-2;

Angevine and Sidman, 1961; Rakic, 1988; Bayer and Altman, 1995; Noctor et al., 2004; Miyata et al., 2004). Although this region is generally called marginal zone or cortical plate in the developing stage of telencephalon, I call it differentiating field (DF) in this paper.

Environmental stresses and stimuli can disturb the process of development, i.e. proliferation, migration, and differentiation of neural cells, in the fetal brain (Fig. I-1; Rodier, 1995; Mendola et al., 2000; Costa et al., 2004). For example, cytotoxic stresses induce excessive cell death and suppress cell proliferation in the developing brain (Katayama et al., 2002, 2005; Ueno et al., 2002a, b, c, 2005; Semont et al., 2004). The balance between proliferation and cell death is important for correct development of the brain (Oppenheim, 1991; Blaschke et al., 1996; Thomaidou et al., 1997; Kuida et al., 1996), so this damage causes structural abnormalities such as reduction in brain size, disorganization of cortical lamina, and dilatation of the ventricles (Fig. I-1; Zhang et al., 1995; Sun et al., 1999; Katayama et al., 2000; Kitamura et al., 2001; Furukawa et al., 2004).

5-Azacytidine (5AzC) and 5-aza-2'-deoxycytidine are agents that have two characteristic effects that interfere with the brain development, i.e. disturbance of DNA methylation (Constantinidis et al., 1977; Jones and Taylor, 1980; Charache et al., 1983; Ley et al., 1982; Bender et al., 1998; Egger et al., 2004; Claus et al., 2005) and DNA damage (Santi et al., 1984; Michalowsky and Jones, 1987; Juttermann et al., 1994; Ferguson et al., 1997; Zhu et al., 2004; Oka et al., 2005) (Fig. I-3). During the development of the CNS as well as other organ systems, DNA methylation is a key step

for regulating gene expression (Sun et al., 2003), and agents such as 5AzC may disturb gene expression and subsequent organogenesis through their DNA demethylating effects. Both agents are also thought to act as a DNA damaging agent (Juttermann et al., 1994; Karpf et al., 2001), and DNA damage causes serious abnormalities in the developing brain (Gao et al., 1998; Vinson and Hales, 2002; D'Sa et al., 2003). Indeed, 5AzC is known as a teratogen, and when it is administered into a pregnant mouse or rat, malformations are induced in the neonatal brain (Langmann and Shimada, 1971; Rodier et al., 1979; Schmahl et al., 1984; Vlahovic et al., 1999). It is further supposed that induction of excessive apoptosis to the neural cells in the developing fetal brain causes neonatal abnormalities (Hossain et al., 1995; Lu et al., 1998).

Although it is demonstrated that cytotoxic stresses induce damage such as cell death and inhibition of proliferation in the developing brain, the mechanisms of chemical-induced toxicity in the developing neural cells remain unclear (Fig. I-1). In the present study, I exposed fetal rat brains to 5AzC to examine the mechanisms of 5AzC-induced toxicity in the developing fetal brain. In chapter 1, the toxicity of 5AzC in the developing brain was examined, and it was demonstrated that 5AzC induced excessive apoptosis and cell cycle arrest to the neural progenitor cells. In chapter 2, to seek the molecular mechanisms of 5AzC-induced apoptosis and cell cycle arrest, I investigated the role of p53, a key molecule in response to DNA damage, and cell cycle checkpoint proteins. Here, I showed that 5AzC-induced apoptosis was mediated by p53, possibly, in response to 5AzC-induced DNA damage, and cell cycle arrest was independent of p53.

Besides the mechanisms of 5AzC-induced toxicity, the process lying between the fetal brain damage and the malformation after birth is still unclear (Fig. I-1). Even if the fetal brain suffers damage, most of the structures of the brain remain after birth, while some abnormalities are included (Fig. I-1). Therefore, it is supposed that repair process is induced after the damage. In chapter 3, to clarify how the developing brain responds and adapts to the damaged tissue, the repair process after the 5AzC-induced injury was examined. I revealed that the developing brain has a capacity to repair the chemical-induced damage with expression of various genes, and microglia aid the repair process.

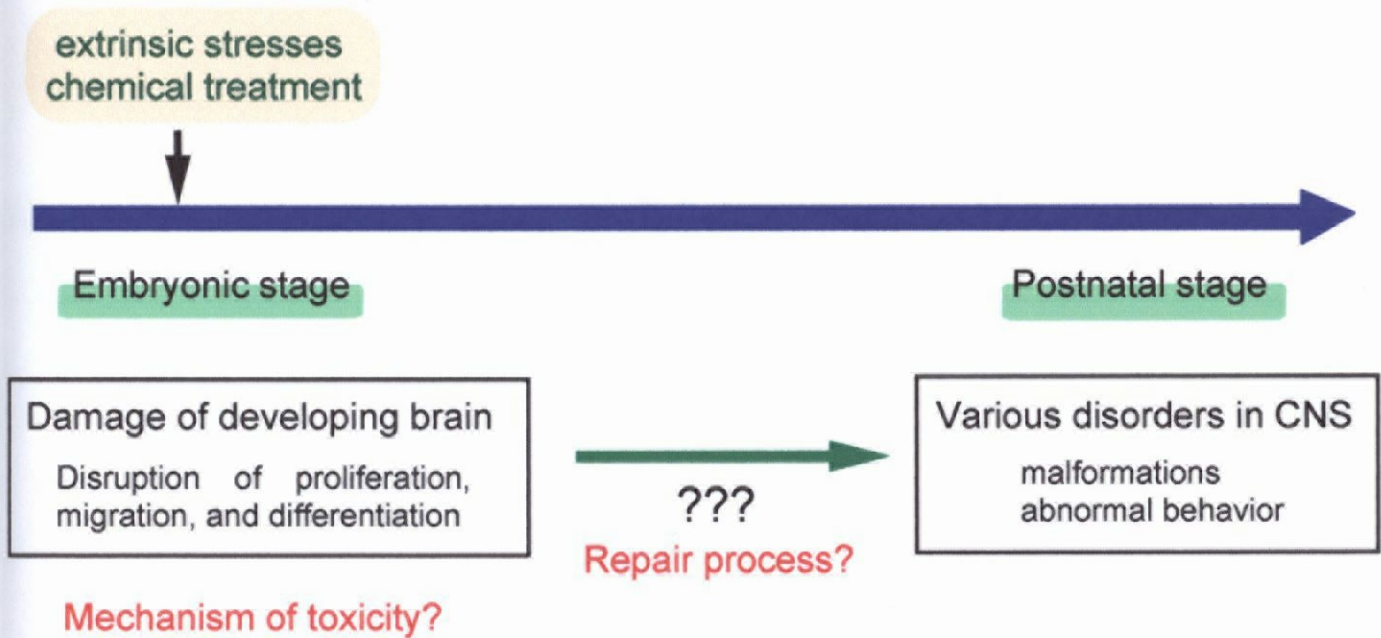


Fig. I-1. Damage of the developing brain by chemical administration. Extrinsic stresses such as cytotoxic chemical treatment in embryonic stage disturb the processes of brain development, i.e. proliferation, migration, and differentiation. This leads to various CNS disorders such as malformation and behavioral disabilities. It remains unclear how developing neural cells are damaged by these stresses in embryonic stage. The process lying between the fetal brain damage and the malformations after birth also is unclear. It is supposed that a certain repair or regenerating processes are involved. The aim of this study is to clarify the mechanism of the chemical-induced toxicity in the developing fetal brain and subsequent presumptive repair process.

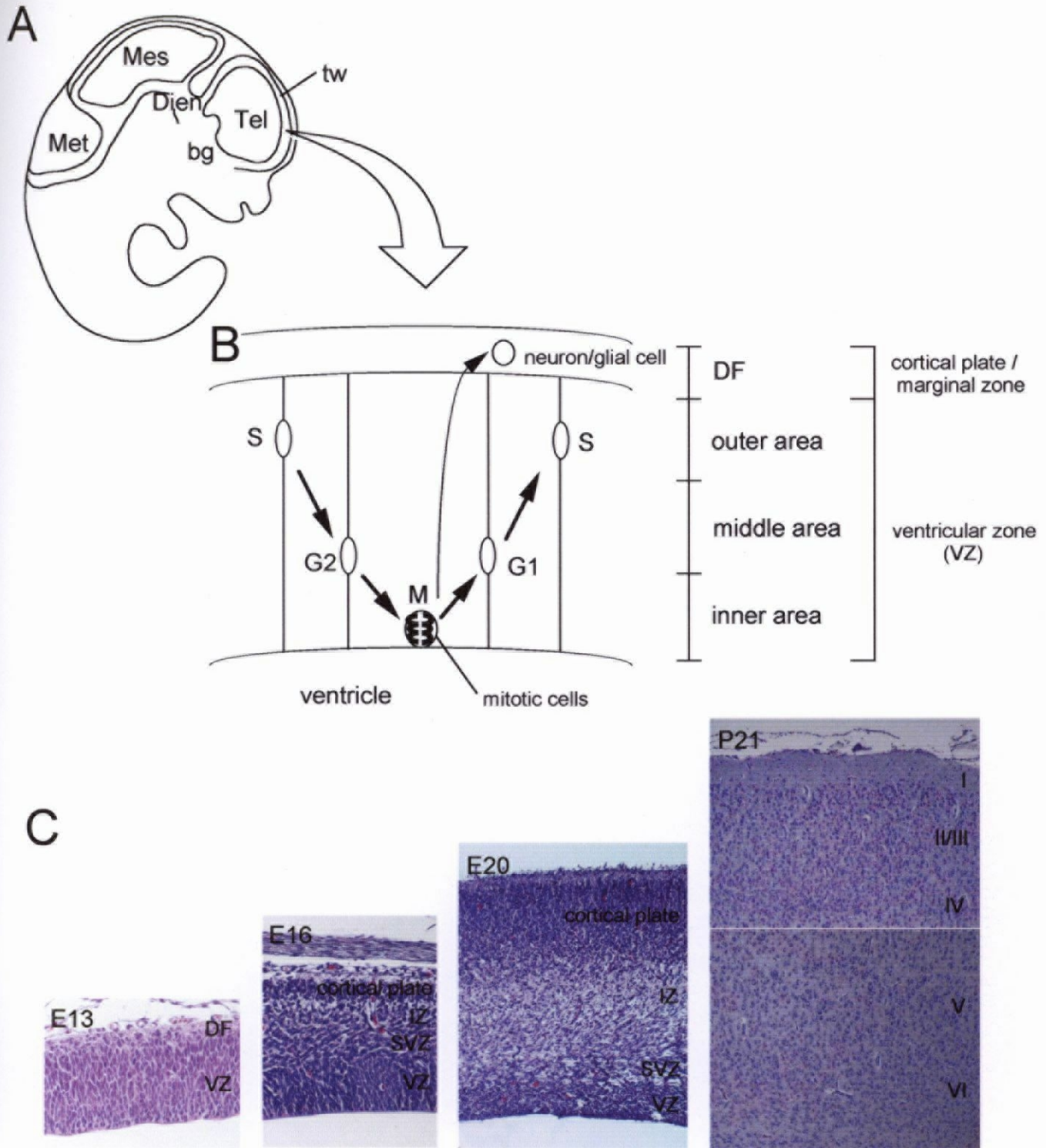


Fig. I-2. Development of rat fetal brain. A: Schematic figure of rat fetal brain from embryonic day (E)13 to 15. The brain consists of four major parts, telencephalon (Tel), diencephalon (Dien), mesencephalon (Mes), and metencephalon (Met). Telencephalic wall (tw) and basal ganglia (bg) are included in telencephalon. B: Telencephalic wall of a rat fetus. Neural progenitor cells proliferate in the ventricular zone (VZ), where their nuclei undergo interkinetic nuclear migration in which they migrate up and down correlating with cell cycle phases. After mitosis, some cells leave the VZ and differentiate into neurons or glial cells in the differentiating field (DF) which is generally called marginal zone or cortical plate. In this study, I divided telencephalic wall into 5 areas (DF, outer area, middle area, inner area, and mitotic cells) to show the localization of neural cells. C: Histology of telencephalic development in rat from E13 to postnatal day (P) 21. Hematoxylin and eosin staining (HE). At E16, subventricular zone, a secondary proliferative zone, is formed. Postmitotic cells migrate through the intermediate zone (IZ) and form cortical plate, where neurons form cortex including 6 layers in adulthood (P21).

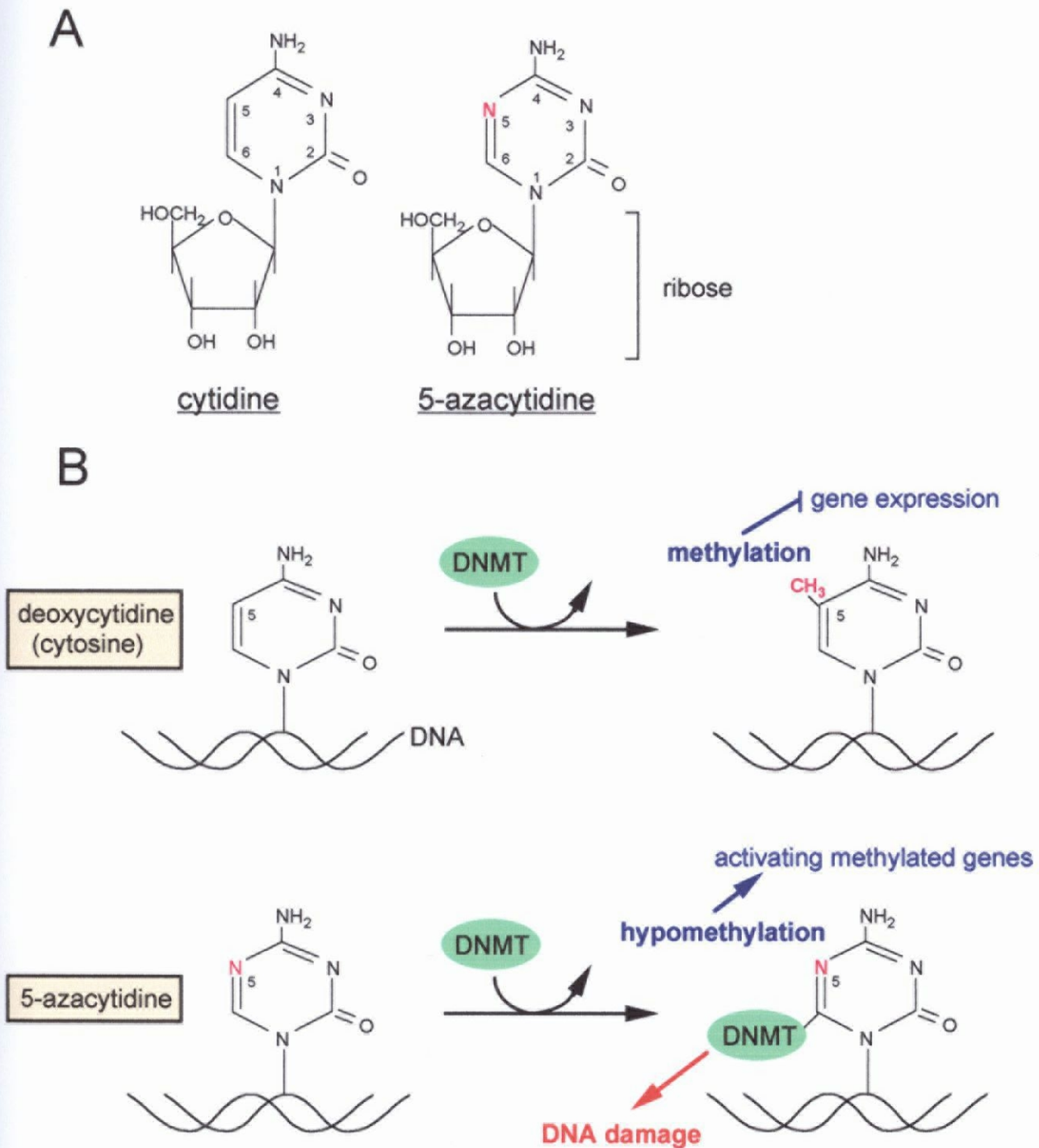


Fig. I-3. The structure and cellular effects of 5-azacytidine (5AzC). A: 5AzC is a cytidine analogue which possesses nitrogen atom instead of carbon atom at the 5 position of pyrimidine ring. B: Cytosine in the promotor region of DNA can be methylated by DNA methyltransferase (DNMT), which suppresses gene expression. 5AzC is incorporated into DNA, and inhibits methylation (hypomethylation). Hypomethylation activates methylated 'sleeping' genes. On the other hand, DNMT forms covalent bond with 5AzC, which leads cells to DNA damage.

## **Chapter 1**

# **5-Azacytidine (5AzC)-induced Toxicity in the Developing Fetal Brain : Cell Death and Cell Cycle Arrest**

## **Introduction**

The balance between proliferation and cell death is important for correct development of the brain (Oppenheim, 1991; Blaschke et al., 1996; Thomaidou et al., 1997; Kuida et al., 1996). Cytotoxic stresses affect cell viability and proliferation, which lead to abnormal brain development (Zhang et al., 1995; Sun et al., 1999; Katayama et al., 2000; Kitamura et al., 2001; Furukawa et al., 2004).

As described in General Introduction, 5AzC is known as a teratogen, and when it is administered into a pregnant mouse or rat, malformations are induced in the central nervous system (Langmann and Shimada, 1971; Rodier et al., 1979; Schmahl et al., 1984; Vlahovic et al., 1999), possibly due to induction of excess apoptosis in the developing fetal brain (Hossain et al., 1995; Lu et al., 1998). Although these studies reported histological changes, it remains unclear how neural cells in the fetal brain react toward extrinsic stresses, like 5AzC, especially regarding the regulation of proliferation and cell death during developing stage of the organ.

In this chapter, fetal rat brains were exposed to 5AzC and responses of the neural progenitor cells to 5AzC-treatment were examined, focusing on the effects on apoptosis and cell cycle kinetics to find a clue for clarifying the detailed mechanisms of 5AzC-induced damage. First, the histopathological changes were examined in the 5AzC-treated developing brain, and it was found that apoptosis and alteration in proliferation occurred. Then, using flow cytometric methods, the alterations in cell cycle distribution were investigated and the cell cycle position of apoptotic cells was assessed. Further, the alteration of nuclear migration of neural progenitor cells, which closely

correlated with their cell cycle progression was evaluated (Fig. I-2B). I found that cell cycle arrest and cell death are included in 5AzC-induced damage in the developing brain.

## **Materials and methods**

All procedures were approved by the Animal Care and Use Committee of the Graduate School of Agricultural and Life Sciences, The University of Tokyo.

### **Animals**

Pregnant Jcl:Wistar rats were obtained from Japan CLEA, Tokyo, Japan. Animals were kept in isolated cages under a controlled condition ( $23\pm 2$  °C with  $55\pm 5$  % humidity and a 14-h light / 10-h dark cycle) and fed commercial pellets (MF; Oriental Yeast, Tokyo, Japan) and water *ad libitum*.

### **Chemicals**

5AzC and 5-bromo-2'-deoxyuridine (BrdU) were obtained from Sigma (St. Louis, MO).

### **Experimental designs**

On day 13 of gestation, pregnant rats were injected intraperitoneally (i.p.) with 10 mg/kg of 5AzC and then euthanized at 1, 3, 6, 9, 12 and 24 h after treatment. The dose was selected according to the results of a previous study, in which 10 mg/kg of 5AzC

caused high induction of neural cell apoptosis and low fetal mortality (Lu et al., 1998). As controls, pregnant rats were injected with an equivalent volume of saline and euthanized at 1, 3, 6, 9, 12 and 24 h after treatment. Collected fetuses underwent histopathological examination and cell cycle analyses.

### **Histopathology and immunohistochemistry**

Collected fetuses were fixed in 10% neutral-buffered formalin and embedded in paraffin. Paraffin sections (thickness, 4  $\mu\text{m}$ ) were stained with hematoxylin and eosin (HE) for histopathological examination. The dorsal telencephalic wall was mainly examined. Some of the sections underwent immunohistochemical staining for cleaved caspase-3, phospho-histone H3 and BrdU by the LSAB method with streptavidin (Dako, Carpinteria, CA). Rabbit anti-cleaved caspase-3 polyclonal antibody (Cell Signaling Technology, Beverly, MA), rabbit anti-phospho-histone H3 polyclonal antibody (Cell Signaling Technology), and mouse anti-BrdU monoclonal antibody (1:100; Dako) were used as the primary antibodies, and biotin-labeled goat anti-rabbit and anti-mouse IgG (Kirkegaard & Perry, Gaithersburg, MD) as the secondary antibodies. The sections for phospho-histone H3 and cleaved caspase-3 were immersed in 10 mM citrate buffer and heated for 10 min at 120 °C in autoclave. The sections for BrdU were pretreated with 0.1% trypsin solution and 1 mol/l HCl. The positive signals were visualized using a peroxidase–diaminobenzidine (DAB) reaction, and then the sections were counterstained with methyl green.

### **TUNEL method**

Cells with DNA fragmentation (apoptotic cells) were detected by the TUNEL method (Gavrieli et al., 1992), using an apoptosis detection kit (Apop Tag; Chemicon, Temecula, CA). In brief, multiple fragmented DNA 3'-OH ends on each fetal section were labeled with digoxigenin-dUTP in the presence of terminal deoxynucleotidyl transferase (TdT). Peroxidase-conjugated anti-digoxigenin antibody was then reacted with the sections. Apoptotic nuclei were visualized by a peroxidase-DAB reaction, and sections were then counterstained with methyl green.

### **Electron microscopy**

For transmission electron microscopic examination, small pieces of fetal heads obtained at 6 h and 12 h after treatment were fixed in 2% glutaraldehyde, 2% paraformaldehyde / 0.1M phosphate buffer (PB) for overnight, and postfixed in 1% osmium tetroxide / 0.2M PB for 2.5 h. After dehydration through an ascending ethanol series and propylene oxide, tissues were embedded in Epok 812 resin (Oken, Tokyo, Japan). Semithin sections were stained with toluidine blue for light microscopic examination. Ultrathin sections were double-stained with uranyl acetate and lead citrate, and observed under a JEOL-1200EX electron microscope (JEOL, Tokyo, Japan).

### **Treatments of BrdU for detection of S-phase cells**

The changes in the number of S phase cells in the fetal brain were examined.

Pregnant rats on day 13 of gestation were injected with 10 mg/kg of 5AzC i.p., and were euthanized at 1, 3, 6, 9, 12, and 24 h after treatment, respectively. The rats were injected with 20 mg/kg of BrdU at 1 hour before sacrifice. As controls, pregnant rats were injected with an equivalent volume of saline in the same way, and were euthanized at 1, 3, 6, 9, 12, and 24 h after treatment, respectively. The rats were injected with 20mg/kg of BrdU at 1 hour before sacrifice.

### **Cell cycle analysis**

Telencephalons of two or three fetuses from each dam (1 to 12 h after treatment, and controls) were obtained carefully under stereoscopic microscopy, and then prepared for flow cytometric analysis. The cells isolated from the telencephalons were resuspended in HBSS. The concentration of the resuspended cells was adjusted to  $1-2 \times 10^6$ . They were centrifuged for 5 min at 1500 g at 4°C, and the supernatant was discarded. After being washed in Dulbecco's PBS (dPBS), the cells were fixed in 70% ethanol at 4°C overnight. Cells then were washed in dPBS and incubated with ribonuclease A (RNase A; 250 µg/ml, Sigma) for 40 min at 37°C. Cells were stained with propidium iodide (PI; 50 µg/ml, Sigma) for 30 min on ice. Cell cycle analysis was performed using the FACS Callibur system (Becton Dickinson, Mountain View, CA), and cell cycle distribution was analyzed using the Cell Quest program (Becton Dickinson).

### **Treatments of BrdU for detecting cell cycle transition and migration**

Pregnant rats on day 13 of gestation were injected i.p. with 10 mg/kg of 5AzC and

20 mg/kg of BrdU concurrently and then euthanized at 1, 3, 6, 9, 12 and 24 h after treatment. As controls, pregnant rats were injected only with BrdU and euthanized at 1, 3, 6, 9, 12, and 24 h after treatment. Collected fetuses underwent flow cytometric analysis to investigate the transition of BrdU-incorporated cells in the cell cycle and immunohistochemistry to detect nuclear migration.

### **Detection of BrdU-positive cells in the cell cycle**

Cells isolated from two or three fetal telencephalons were resuspended and then washed and fixed using the same method described in cell cycle analysis. After being fixed in 70% ethanol, the cells were washed with dPBS and then resuspended for 30 min at room temperature (RT) in 2 M HCl containing 0.5% Triton X-100. After being neutralized in 0.1 M  $\text{Na}_2\text{B}_4\text{O}_7$ , the cells were incubated with FITC-labeled anti-BrdU monoclonal antibody (Pharmingen, San Diego, CA) for 30 min at RT. They then were resuspended in dPBS containing PI (10  $\mu\text{g}/\text{ml}$ ) for 30 min on ice and analyzed using the FACS Callibur system and Cell Quest program (Becton Dickinson).

### **Detection of fragmented DNA in the cell cycle**

Fragmented DNA was detected with an APO-BrdU Kit (Pharmingen). The manufacturer's protocol was followed with minor modifications. Cells were isolated from three rat fetal telencephalons from each dam (9 and 12 h after treatment, and controls) as for cell cycle analysis, and first fixed in 1% paraformaldehyde (PFA) in dPBS for 15 min on ice. After being washed with dPBS, they were fixed in 70%

ethanol at 4°C for one or two overnights. Cells then were washed in the Wash Buffer from the kit and incubated in the DNA Labeling Solution for 60 min at 37°C. In this solution, the multiple fragmented DNA 3'-OH ends in the nuclei were labeled with BrdUTP in the presence of TdT. After being washed in Rinse Buffer, cells were incubated for 30 min at RT in Antibody Staining Solution containing FITC-labeled anti-BrdU antibody and then stained with PI/RNase A solution for 30 min at RT. FITC-positive apoptotic cells were detected and analyzed using the FACS Callibur system and Cell Quest program (Becton Dickinson).

## **Results**

### **Histopathological changes**

Administration of 5AzC (10 mg/kg) into pregnant rats on day 13 of gestation induced histopathological changes such as accumulation of mitotic cells and apoptosis in the fetal brain.

First, to investigate the alteration of proliferation, mitotic cells which were positive for phospho-histone H3, a marker of mitosis, were counted. Although this antigen is also present in late G2 phase, only the phospho-histone-H3 positive cells which have mitotic figures were counted. At 6 h after 5AzC-treatment, the number of mitotic cells increased in the VZ along the ventricular surface (Fig. 1-1A, B). These cells decreased in number after 6 h (Fig. 1-1A, B). Mitotic figures showed pleomorphic ultrastructural pictures with chromosomal abnormalities such as multiple collections of chromatin through the cytoplasm, asymmetric separation of chromosomes, lagging chromosomes,

and dispersed large chromatin masses bounded by nuclear membranes (Fig. 1-1C).

From 6 to 24 h, the number of pyknotic cells, which had morphological characteristics of apoptotic cells, increased among the neural progenitor cells in the VZ. Apoptotic cells showed pyknosis or karyorrhexis on the HE section (Fig. 1-2A-a), and the nuclei of these cells were strongly stained with TUNEL method (Fig. 1-2A-b-e). Immunohistochemically, the pyknotic cells were stained positively for cleaved caspase-3 (Fig. 1-2A-f-j), which is known to be involved in neural cell apoptosis during development as well as in the apoptosis of neurons induced by DNA-damaging agents (Kuida et al., 1996; Keramaris et al., 2000). TUNEL-positive apoptotic cells appeared remarkably at 9 h in the VZ (Fig. 1-2A-c). The TUNEL index peaked at 12 h and slightly decreased at 24 h (Fig. 1-2A, B). At 9 and 12 h, apoptotic cells were observed in the VZ, whereas at 24 h, apoptotic cells were found in the DF, the upper area of VZ, where neuroepithelial cells differentiate into neurons (Fig. 1-2A-c-e). Apoptosis occurred similarly in all fetal brain regions examined, i.e. telencephalon, diencephalon, mesencephalon and metencephalon (these brain regions are represented in Fig. I-2A) (Fig. 1-2B), so all the subsequent analyses were undertaken in the telencephalon. Electron microscopically, condensation of nuclear chromatin, margination of condensed chromatin along the nuclear membrane and/or shrinkage of the cell body were seen (Fig. 1-2C). Some cell nuclei were fragmented into small pieces, which were ingested by adjacent cells (Fig. 1-2C-c). These ultrastructural findings were consistent with those of apoptosis.

## **Sequential changes in the number of BrdU-labeled S phase cells after 5AzC administration**

After 5AzC was injected into pregnant rats on day 13 of gestation, BrdU (20 mg/kg) was injected at 1 h before sacrifice. Then, the number of BrdU-positive cells which correspond to S phase cells was sequentially examined. Until 9 h, there were no significant differences between the control and the 5AzC-treated groups (Fig. 1-3). At 12 h, the number of BrdU-positive cells significantly decreased in the 5AzC-treated groups as compared to that in the control group (Fig. 1-3A-a, f, B), suggesting that cell cycle arrest occurred at a certain phase before the S phase.

## **Cell cycle analysis**

The alteration of cell cycle was then analyzed using flow cytometry because some disturbances in cell cycle regulation were indicated in the previous histopathological observations. In embryonic day (E) 12 to E13 mice, about 70% of cells in the fetal telencephalon are neural progenitor cells (D'Sa-Eipper and Roth, 2000), so it was considered that the cells analyzed reflected the cell cycle distribution of neural progenitor cells (Fig. 1-4). Further, most of the neural progenitor cells analyzed were thought to localize in the VZ, rather than the subventricular zone (SVZ), the other area where neural progenitor cells proliferate, because the SVZ is not yet prominent in E13 rat (see Fig. 1-2, 1-1A, 1-2A).

The cell cycle distribution from 1 to 3 h after 5AzC-treatment did not markedly differ from that of the control (Fig. 1-4). At 6 h, the number of cells in G2/M phase

increased (control,  $8.8 \pm 0.7\%$ ; 5AzC,  $15.0 \pm 0.9\%$ ) and that in G0/G1 decreased (control,  $72.5 \pm 1.4\%$ ; 5AzC,  $61.6 \pm 1.0\%$ ). This phenomenon likely relates to the accumulation of mitotic cells along the ventricle, as observed in the histopathological analysis (Fig. 1-1A-a, e, B). At 9 h, the number of cells in G2/M further increased ( $16.1 \pm 0.6\%$ ), that of S phase increased slightly, and that of G0/G1 decreased. These results suggest that neural progenitor cells were arrested at the S/G2 and G2/M transitions. Although phospho-histone H3-positive cells with mitotic figures decreased at 9 h compared to 6 h (Fig. 1-1A, B), the number of cells in the G2/M phase increased at 9 h. It indicates that at 9 h, G2 arrest occurred while the degree of mitotic arrest decreased. Further, apoptotic cells began to appear in the sub-G1 area from 6 to 9 h after 5AzC-treatment. At 12 h, the number of cells accumulated in G2/M was reduced, the number of cells in the S phase decreased, and that of G0/G1 phase increased. At the same time, the number of apoptotic cells remarkably increased ( $15.8 \pm 3.2\%$ ). In light of these results, the G2/M arrest appeared to have been released and the cells shifted to G0/G1 after mitosis, or to apoptosis.

### **Detection of BrdU-positive cells in the cell cycle**

To confirm that cells shifted from arrest at G2/M and either entered G0/G1 or became apoptotic, I injected 5AzC and BrdU concurrently and used a flow cytometry to investigate the cell cycle transition of 5AzC-treated neural progenitor cells. 5AzC and BrdU both are incorporated into DNA during the S phase of the cell cycle.

In the BrdU-only control group, BrdU first was incorporated into S-phase cells at 1

h after treatment (Fig. 1-5). At 3 h, the BrdU-incorporated cells had transited from S to G2/M phase, and some had entered G0/G1. At 6 h, most of the BrdU-positive cells had exited S phase and were in G2/M or G0/G1. At 9 h, some BrdU-positive cells had re-entered S phase, and most of them had returned to S phase by 12 h. The duration of a single complete cell cycle is thought to be at least 12 h, an assumption that is supported by the previous reports (von Waechter and Jaensch, 1972; Takahashi et al., 1995).

When 5AzC was injected with BrdU, BrdU-incorporated cells transited from S to G2/M phase during 1 h through 3 h (Fig. 1-5). At 6 h, more 5AzC-treated cells than control cells were still in G2/M (control,  $16.5 \pm 3.4\%$ ; 5AzC,  $43.6 \pm 6.7\%$ ). Many of the G2/M-arrested cells likely were in M phase, because most of the abnormal mitotic cells were BrdU-positive as described below (Fig. 1-6A-i). At 9 h, most of them still remained in the G2/M phase (control,  $5.3 \pm 1.9\%$ ; 5AzC,  $23.9 \pm 2.7\%$ ), but some cells had moved to G0/G1. As shown in the next nuclear migration-study, a small number of BrdU-positive cells (about 4 %) were mitotic cells at 9 h (Fig. 1-6A-j), suggesting that G2 arrest occurred in this period. Further, some BrdU-positive cells had undergone apoptosis, as demonstrated by the increase in the sub-G1 area ( $13.3 \pm 3.3\%$ ). At 12 h, the cells moved to G0/G1 or to the sub-G1 area, which contained apoptotic cells. These results indicate that 5AzC-treated neural progenitor cells underwent M arrest at 6 h and G2 arrest at 9 h, after which they either entered G0/G1 phase or became apoptotic.

## **Nuclear migration of neural progenitor cells**

Because cell cycle progression of neural progenitor cells is closely related to the nuclear migration (Fig. I-2B), 5AzC and BrdU were injected into pregnant rats, and then the distribution of BrdU-positive nuclei in the VZ was examined by using immunohistochemical staining to determine whether 5AzC treatment induced changes in nuclear migration patterns. To show the sites of BrdU-positive cells, the telencephalic wall was divided into 5 areas (DF, outer area, middle area, inner area, and mitotic cells; Fig. I-2B). In the control fetuses, BrdU-injection caused no significant histopathological changes.

At 1 h after treatment, BrdU-positive cells were mainly observed in the outer area of the VZ in both groups (Fig. 1-6A-a, g). In the control group, BrdU-positive signals were first observed at 3 h in mitotic cells. They increased in the inner area and decreased in the outer area at 3 h (Fig. 1-6b). At 6 h, many BrdU-positive cells were seen in the inner area, while the number in the outer area reached the lowest level (Fig. 1-6A-c). At 9 h, the number of BrdU-positive cells reached the peak level in the middle area, and it began to increase in the outer area. On the other hand, BrdU-positive signals disappeared in mitotic cells (Fig. 1-6A-d). At 12 h, the number of BrdU-positive cells in the outer area reached the peak again, while it decreased in the middle and inner area (Fig. 1-6A-e). At 24 h, the number of BrdU-positive cells decreased in the outer, middle, and inner area (Fig. 1-6A-f), and it increased in the DF from 6 to 24 h. Thus, BrdU was incorporated mainly in neural progenitor cells in the outer area at 1 h, and BrdU-incorporated cells migrated through the middle to inner area,

devided along the ventricle from 3 to 6 h, moved again through the inner to middle area from 6 to 9 h, and reached the outer area at 12 h. This migration pattern shows the well-known interkinetic nuclear migration (Fig. I-2B). Further, the duration of a single complete cell cycle is thought to be at least 12 h, which is consistent with the results in the analyses by flow cytometry (Fig. 1-5).

In the 5AzC-treated group, BrdU-positive cells in mitotic cells were first seen at 3 h (Fig. 1-6A-h), like in the control group (Fig. 1-6A-b). At 6 h, a prominent accumulation of mitotic cells was observed along the ventricle as shown in histopathological study (Fig. 1-1), and BrdU-positive signals were seen in most of these mitotic cells (Fig. 1-6A-i). BrdU-positive cells significantly increased in mitotic cells, while they decreased in the middle area (Fig. 1-6A-i, B). At 9 h, BrdU-positive cells significantly increased in the inner area, while they decreased in the middle and outer areas (Fig. 1-6A-j). It is suggested that the delay in migration at this time point relates to the cell cycle arrest at G2 phase (Fig. 1-4, 1-5). At 12 h, BrdU-positive cells significantly decreased in the outer area and the DF (Fig. 1-6A-k, B). BrdU-positive signals were observed in some pyknotic cells at 9 and 12 h (Fig. 1-6A-j, k), and in most of pyknotic cells at 24 h (Fig. 1-6A-l), which were seen in the DF.

### **Cell cycle position of cells undergoing apoptosis**

I then sought to confirm whether the 5AzC-treated apoptotic cells had died before or after mitosis. The results of cell cycle analysis were consistent with those of histopathological examination, showing that apoptotic cells began to increase at 9 h and

that the number peaked at 12 h after 5AzC-treatment (Fig. 1-2B, 1-4). To clarify at which cell cycle phase 5AzC-treated neural progenitor cells undergo cell death, the presence of DNA strand breaks in cells versus their DNA content was assessed using flow cytometry. The cells first were fixed with PFA, which prevents apoptotic cells from losing their DNA fragments (loss of DNA fragments causes the cells to stain as a sub-G1 population) (Gorczyca et al., 1993; Murakami et al., 1995). In this way the apoptotic cells with the DNA contents indicative of G0/G1, S, or G2/M phases can be detected, thus clarifying during which phase the cells died.

The results of the flow cytometric analysis of the paraformaldehyde-fixed cells are shown in Figure 1-7. From 9 to 12 h after the treatment, most of the cells undergoing apoptosis were in G0/G1 phase (9 h,  $65.0 \pm 5.8\%$ ; 12 h,  $56.6 \pm 3.7\%$ ), although some were in G2/M and S phases. At 12 h, the ratio of apoptotic cells in the G0/G1 phase decreased and that in the G2/M phase increased slightly. The current findings suggest that apoptosis is predominantly induced after the mitosis, but some cells die before.

## **Discussion**

In the present study, it was shown that 5AzC induced neural cell death by apoptosis and G2/M arrest. The mechanism of 5AzC-induced toxicity in the developing fetal brain was summarized in Fig. 1-8. Here, I will discuss what occurred in the neural cells when 5AzC was treated, focusing on apoptosis and cell cycle regulation.

### **Induction of apoptosis**

In this study, it was confirmed that 5AzC induced neural cell death by apoptosis, because most of pyknotic cells induced by 5AzC were TUNEL- and cleaved caspase 3-positive, and had ultrastructural characteristics of apoptosis. 5AzC-treatment at prenatal days induces apoptosis in the fetal brain (Hossain et al., 1995; Lu et al., 1998) as confirmed in the present study, and it reduces the weight and length of postnatal brain, in which the number of neurons decreases (Langman and Shimada, 1971; Rodier et al., 1979). In ethylnitrosourea (ENU)-treated fetuses, Katayama et al. (2000) reported that excess cell death by apoptosis has a close relation to anomalies. These findings suggest that 5AzC-induced malformations may also be resulted from decreased number of neural cells by apoptosis.

The occurrence of apoptosis was also observed in the central nervous system of rat fetuses following radiation (Borovitskaya et al., 1996), ENU administration (Katayama et al., 2001), or AraC administration (Yamauchi et al., 2004). This suggests that neural progenitor cells are able to respond to genotoxic effects, resulting in apoptotic cell death.

In the present study, apoptotic cells appeared at 9 h, and the number peaked at 12 h. In other models, the number of apoptotic cells peaked at 3 to 5 h by radiation (Borovitskaya et al., 1996) and 3 to 12 h by ENU or AraC-treatment (Katayama et al., 2001, Yamauchi et al., 2004), respectively. The peak time was later than those in other models, in spite of the rapid accumulation of 5AzC in the fetal brain (Seifertova et al., 1968; Seifertova et al., 1974) and elimination from the blood of the mother within 1.8 hours (Raska et al., 1965). The late appearance of apoptosis may be reflected by the

nature of 5AzC, or the capacity of neural progenitor cells which repair the 5AzC-induced damage, probably DNA damage or demethylation. It seems that DNA repair process to the 5AzC-induced damage occurred at later stages following S phase at which 5AzC is incorporated, because cell cycle arrest first occurred at G2/M phase, and apoptosis was induced mainly at G0/G1 phase after mitosis or some in G2/M phase.

5AzC or 5-aza-2'-deoxycytidine is incorporated into DNA during DNA replication phase (S phase), and exerts its cell toxicity *via* the DNA hypomethylating effect (Constantinidis et al., 1977; Jones and Taylor, 1980; Charache et al., 1983; Ley et al., 1982; Bender et al., 1998; Egger et al., 2004; Claus et al., 2005) or the direct inhibition of DNA functions: DNA damage (Santi et al., 1984; Michalowsky and Jones, 1987; Juttermann et al., 1994; Ferguson et al., 1997; Zhu et al., 2004; Oka et al., 2005). Although it is still unclear which effect causes apoptotic cell death, it is thought that at least DNA damage was induced in this study, because cell cycle arrest is generally known to occur for repairing the DNA damage. I investigated the molecular mechanism of 5AzC-induced toxicity in the next chapter, and I will show some suggestions regarding with which effect of 5AzC induces apoptosis and cell cycle arrest to the neural progenitor cells.

At 24 h after treatment, most apoptotic cells were observed in the DF, and most of them were BrdU-positive, suggesting that 5AzC-incorporated cells also undergo apoptosis after leaving the cell cycle and migrating to the upper area of the VZ. The cells in the DF, which is generally called marginal zone or cortical plate, have already left the cell cycle in the VZ, and would later differentiate into neurons (Angevine and

Sidman, 1961; Rakic, 1988; Bayer and Altman, 1995; Noctor et al., 2004; Miyata et al., 2004). It is possible that other mechanism is involved in the apoptotic cell death of differentiating neural cells.

### **Cell cycle arrest**

The present results revealed several clues regarding cell cycle regulation of neural progenitor cells in response to 5AzC-induced stresses, which normally proliferate with a characteristic migration—interkinetic nuclear migration (or “elevator movement”) —in the VZ (Sauer and Walker, 1959; Fujita, 1960, 1962, 1963, 2003; Yoshida et al., 1987; Takahashi et al., 1992, 1993; Fig. 1-8). Firstly M, and secondly G2 arrest occurred from 6 to 9 h after 5AzC-treatment. Although mitotic cells decreased at 9 h compared to 6 h (Fig. 1-1A, B), the number of cells in the G2/M phase increased at 9 h (Fig. 1-4). It indicates that at 9 h, G2 arrest occurred while the degree of mitotic arrest decreased. Accumulation of mitotic cells along the ventricle and delay in inward-migration were also observed (Fig. 1-6A-i, j), which would reflect cell cycle arrest at M and G2 phase. Then the number of cells in G1 phase and that of apoptotic cells increased.

At 6 h, a prominent accumulation of mitotic cells showing pleomorphism was observed along the ventricle. Some of mitotic cells seemed to be abnormal ones, although it is difficult to distinguish abnormal mitotic figures from normal ones (Cheville, 1994). Some reports have also shown that 5AzC induces abnormal mitosis including chromosomal aberrations and endoreduplication (Langmann and Shimada, 1971; Flagiello et al., 2002; Nieto et al., 2004; Dodge et al., 2005; Mateos et al., 2005).

Abnormal mitotic figures are also observed in tumor cells, in which, for example, lagging chromosomes at meta and anaphase, chromatin in droplets (Timonen and Therman, 1950), and dispersed chromosome bounded by a nuclear envelope occurred (Henderson and Papadimitriou, 1982). Abnormal mitoses in tumors are induced by several factors including defects in chromosome, centrosome, spindle formation, and mitotic checkpoint (Kops et al., 2005), so it is possible that 5AzC-induced abnormal mitosis also occurred by these defects. On the other hand, M phase arrest is induced by mitotic checkpoint signaling in p53 dependent (Cross et al., 1995) or independent manner (Lanni and Jacks, 1998) when mitosis is disturbed. It is therefore unclear whether increasing number of mitotic cells by 5AzC-treatment is a result from direct defects of mitosis or the effect of mitotic checkpoint. Recently, mitotic catastrophe, a type of cell death occurring during or after mitosis with some mitotic failure, has been proposed (Castedo et al., 2004). Although the definition of this cell death is controversial among researchers, 5AzC-induced abnormal mitosis and subsequent apoptosis might fall into this category. I performed several additional experiments for clarifying the mechanism of 5AzC-induced mitotic abnormalities and discussed these issues in chapter 2.

G2 arrest commonly occurs when DNA damage is induced into cells (Taylor and Stark, 2001; Iliakis et al., 2003). In the 5AzC-treated neural progenitor cells, therefore, DNA damage would cause G2 arrest. It is known that p53 dependent and independent mechanisms are included in G2/M checkpoint (Taylor and Stark, 2001). These molecular mechanisms were investigated in chapter 2.

## **Nuclear migration of neural progenitor cells**

The regulation of the nuclear migration of neural progenitor cells is poorly understood. The “elevator movement” exhibited by the nuclei is thought to be dependent on cell cycle progression (Fig. I-2B). Indeed, most S-phase nuclei are observed in the outer area of VZ which is shown by <sup>3</sup>H-thymidine or BrdU labeling, whereas most mitotic cells are on the ventricular surface (Sauer and Walker, 1959; Fujita, 1960, 1962, 1963; Yoshida et al., 1987; Takahashi et al., 1992, 1993). The nuclear migration of neural progenitor cells was confirmed not only by <sup>3</sup>H-thymidine and BrdU-labeling, but also by time-lapse observations of fluorescently labeled cells (Noctor et al., 2001; Miyata et al., 2001; Tamamaki et al., 2001).

In the present study, it was examined whether this nuclear migration pattern correlated with cell cycle progression, even when cell cycle progression was chemically disrupted. As expected, neural progenitor cells stopped their migration according to their phase of cell cycle arrest. 5AzC-treatment induced M or G2 arrest, and the nuclei of neural progenitor cells stopped their migration along the ventricles and in the inner area of the VZ, where they would normally be located during the M and G2 phase, respectively (Fig. 1-6). It was also shown that ENU or cyclophosphamide (CP) treatment induced S-phase arrest, and the nuclei of neural progenitor cells stopped their migration in the outer area of the VZ, where the nuclei of S-phase cells normally exist (Katayama et al., 2005a; Ueno et al. unpublished data). Although other phase arrests (i.e. G1 phase) were not investigated, it is considered that the same relationship

probably exists between migration and cell cycle at all phases.

These results suggest the presence of a mechanism to connect nuclear migration and cell cycle progression. For example, cell cycle regulators that play a role in the G2 transition might also induce inward nuclear migration. Once the cell cycle regulators stop the G2 transition, they might stop the inward-translocation. The same phenomena are assumed to occur in other cell cycle phases.

It has been shown in *in vitro* studies that the cyclin-dependent kinase inhibitors p21 and p27 regulate not only cell cycle progression, but also cell migration via cytoskeletal reorganization (Fukui et al., 1997; Sun et al., 2001; Diez-Juan et al., 2003; Besson et al., 2004). In the next chapter, I showed that 5AzC-treatment elevated the expression of p21<sup>waf1/cip1</sup>. Thus, there may be some mechanisms by which these cell cycle regulators modify the structure of cytoskeleton to change the nuclear migration. Another candidate gene that links the migration with the cell cycle is  $\beta$ -catenin.  $\beta$ -catenin plays a role in adhesion and proliferation. It is suggested that N-cadherin- $\beta$ -catenin- $\alpha$ -catenin complex, the adherence apparatus connecting the neuroepithelial cells (Takeichi, 1995; Gumbiner, 2005), may be important for the interkinetic nuclear migration (Fujita, 2003). Besides these roles in cell adhesion and migration,  $\beta$ -catenin also regulates the cell cycle as a transcription co-factor that upregulates the expression of several cell cycle-related genes, such as *cyclin D1* and *c-Myc* (He et al., 1998; Tetsu and McCormick, 1999; Shtutman et al., 2001). Indeed,  $\beta$ -catenin controls cell cycle progression in neural progenitor cells (Chenn and Walsh, 2002). The localization and phosphorylation state of  $\beta$ -catenin are changed in each phase of the cell cycle in some

types of cells (Olmeda et al., 2003), suggesting that the role of  $\beta$ -catenin in adhesion and proliferation may be dynamically altered in each phase. Therefore, although the nuclear localization of  $\beta$ -catenin is not clear in neural progenitor cells (Chenn and Walsh, 2002; my unpublished data),  $\beta$ -catenin may connect the cell cycle and migration systems of neural progenitor cells. These two examples suggest a potentially broad mechanism by which cell cycle regulators might induce reorganization of the cytoskeleton and ultimately alter nuclear migration.

The present findings suggest that 5AzC induces apoptosis at multiple cell cycle stages, consistent with the results of another report (Murakami et al., 1995). Together these results suggest that some cells pass from G2/M to G1 phase with completion of correct DNA repair, others enter G1 but undergo apoptosis because of incomplete repair, and still others stay in G2/M to undergo apoptotic cell death (Fig. 1-8B). The cells dying at G1 after mitosis might have died due to mitotic catastrophe, as a result of incomplete mitosis and faulty DNA repair at G2 or S phase (Fig. 1-8B).

Because neural progenitor cells have a high proliferating activity, they are susceptible to many extrinsic stimuli, especially DNA damage. These cells have the potential to repair after these damages via cell cycle arrest and to exclude highly affected cells through the apoptotic process, although the responses of the cells differ slightly depending on the type of DNA damages. For example, ionizing irradiation induces G1 arrest and apoptosis in neural progenitor cells (Semont et al., 2004), whereas ENU induces S arrest and apoptosis (Katayama et al., 2005). Regardless, if

the adverse extrinsic stimulus is sufficiently low to preclude DNA damage or allow its repair, neural progenitor cells can re-engage and proliferate for correct development of the brain after the injury. However, if the stimulus and subsequent DNA damage are high, excess cell death and cell cycle arrest occur. Thus once the balance between proliferation and cell death is highly disturbed, it leads to abnormal brain development and results in malformation of the neonatal brain.

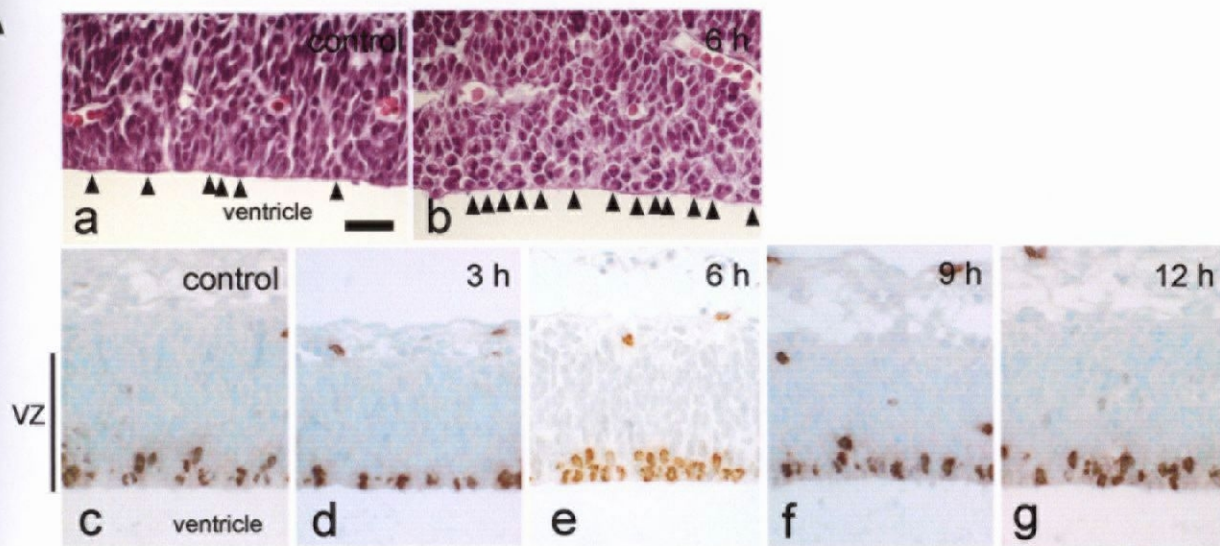
In the next chapter, I further investigated the molecular mechanisms of the regulation of cell cycle and cell death in the 5AzC-treated neural progenitor cells.

## **Summary**

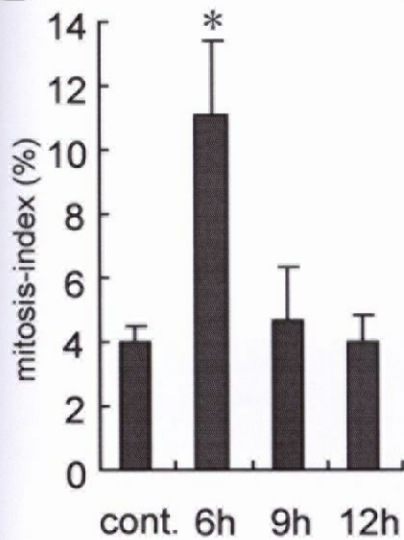
In the developing brain, neural progenitor cells are susceptible to many extrinsic stresses. Pregnant rats were treated with 5AzC, a DNA demethylating and damaging agent, to investigate the cellular responses of the fetal brain, focusing on the regulation of proliferation and cell death. 5AzC first induced the accumulation of cells in abnormal mitosis, G2 phase arrest, and then apoptosis of the neural progenitor cells. Most of the apoptotic cells were in G1 phase. Cell cycle transition studies using BrdU-labeling method suggested that G2/M arrest occurred, after which the cells moved to G1 phase or underwent apoptosis. Further the nuclear migration of neural progenitor cells which is closely related to cell cycle progression delayed as compared to the control migration, and paralleled with cell cycle arrest. The present results indicate that 5AzC induced apoptosis and cell cycle arrest to the neural cells in the developing brain, which would lead to malformations in the neonatal brain.

Throughout brain development, various cell cycle and cell death regulation provide neural progenitor cells with options for defense from DNA damage.

A



B



C

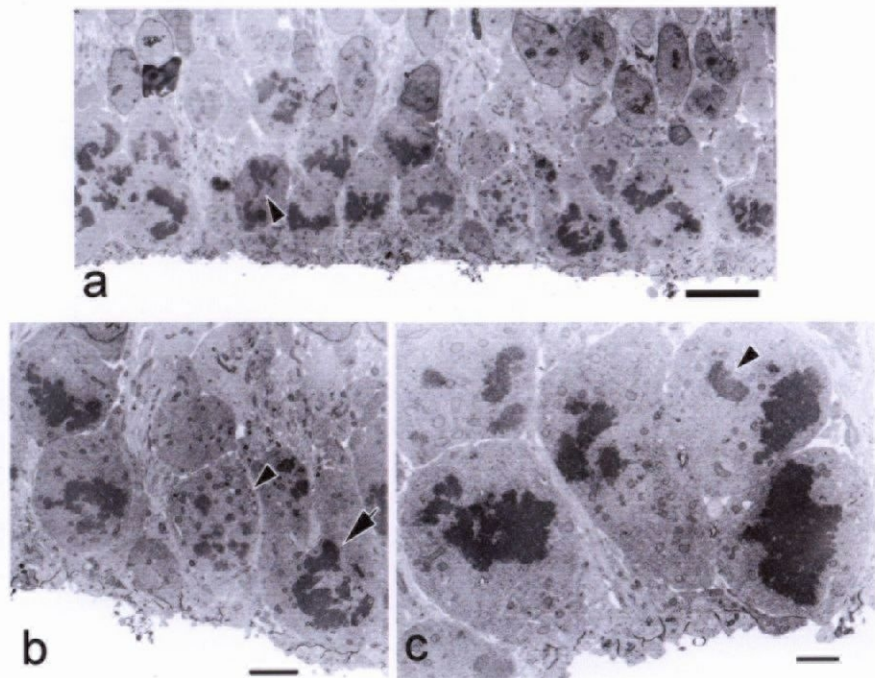


Fig. 1-1. Accumulation of mitotic cells along the lateral ventricle in the telencephalon after 5AzC-treatment. A: Increasing mitotic cells were observed in HE section (a, b; arrowheads) and immunohistochemistry for phospho-histone H3, a marker of mitosis (c-g). a, c: control (12 h), d: 3 h, b, e: 6 h, f: 9 h, g: 12 h after 5AzC-treatment. Scale bar: 50  $\mu\text{m}$ . B: The mitosis-index (%) of neural progenitor cells at the ventricular surface. The indices (%: the number of phospho-histone H3-positive cells with mitotic figures / 500 cells in the VZ) are represented as mean  $\pm$  SD of 3 dams. \*:  $p < 0.05$ ; significantly different from the control (12 h) (Student's *t*-test). Mitotic cells remarkably increased at 6 h and then decreased to the control level. C: Electron micrograph of accumulated mitotic cells. Many cells show pleomorphic mitotic figures in the VZ facing the ventricle (a). In higher magnification of a part of a (b), multiple collections of chromatin through the cytoplasm (arrowhead) and dispersed large chromatin masses bounded by nuclear membranes (arrow) are seen. Lagging chromosomes at metaphase (c: arrowhead) or anaphase (a: arrowhead) are observed. Scale bar: 10  $\mu\text{m}$  (a), 4  $\mu\text{m}$  (b), 2  $\mu\text{m}$  (c).

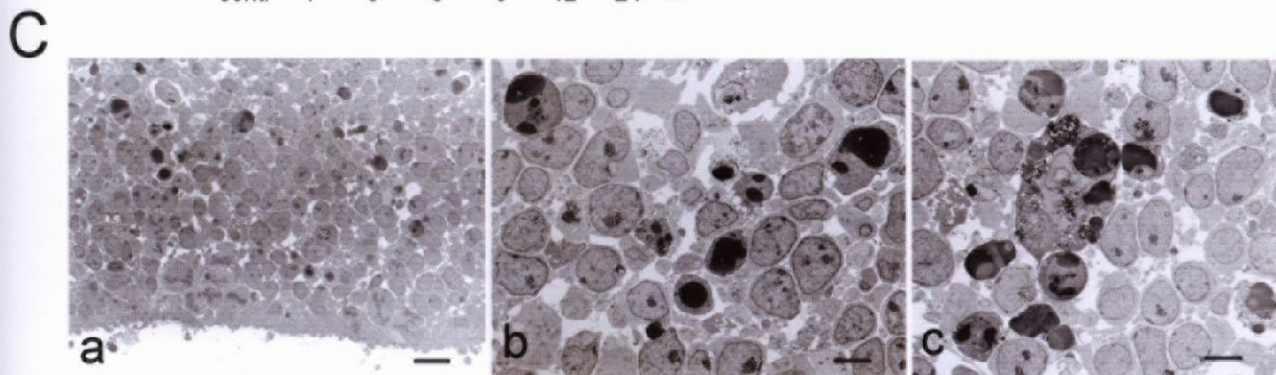
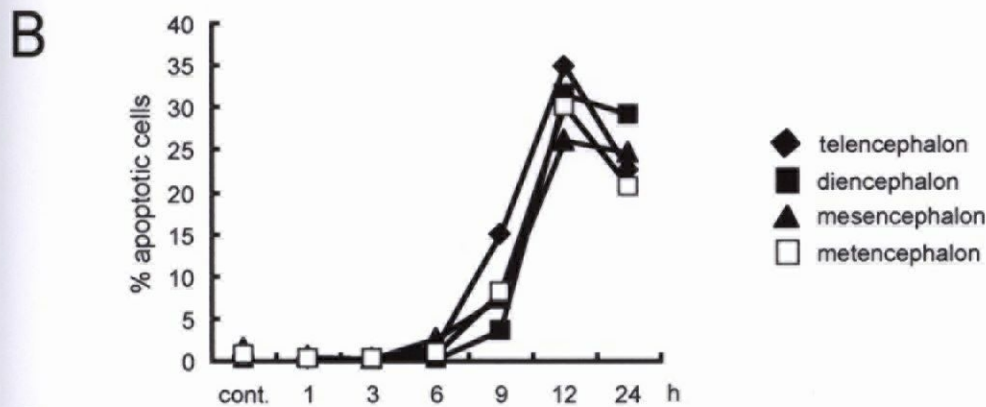
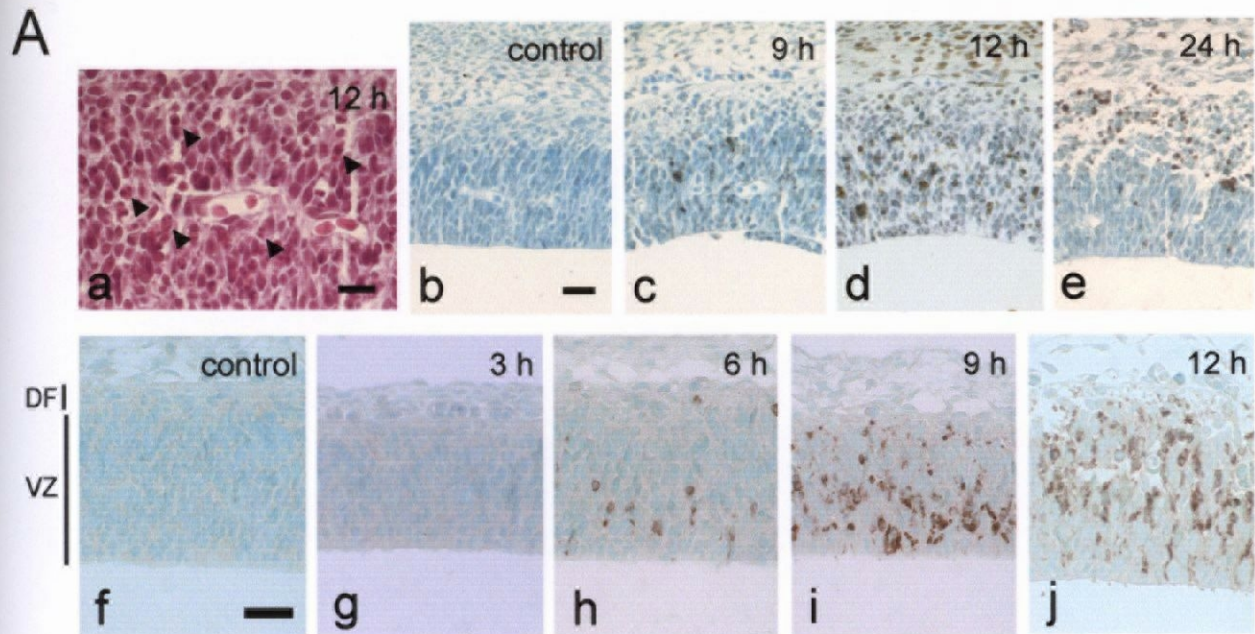
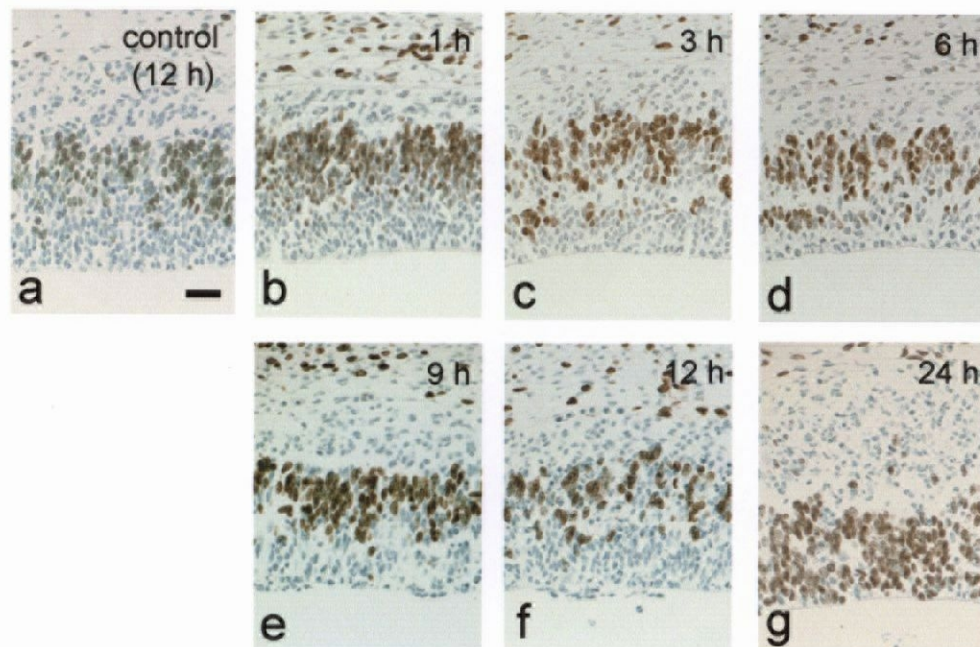


Fig. 1-2. 5AzC-induced apoptotic cell death in the fetal brain. A: Histology of apoptotic cells in the telencephalic wall of 5AzC-treated fetuses. Apoptotic cells show pyknotic or fragmented nuclei on HE section (a: 12 h after treatment; arrowheads), those are TUNEL- (b-e) and cleaved caspase-3 positive (f-j). b, f: control (12 h); g: 3 h; h: 6 h; c, i: 9 h; d, j: 12 h; e: 24 h after 5AzC-treatment. Scale bar: 25  $\mu$ m (a), 50  $\mu$ m (b, f). B: The apoptosis-index (%) of neural cells in four main areas of the brain, telencephalon (◆), diencephalon (■), mesencephalon (▲), and metencephalon (□). The indices (%: the number of TUNEL-positive cells / 500 cells) are represented as the mean of 2 dams. C: Electron micrograph of apoptotic cells in the telencephalic wall at 12 h. Apoptotic cells are localized adjacent to the mitotic cells along the ventricle to the outer area in the VZ (a). Apoptotic cells show condensed or fragmented nuclear chromatin (b), and apoptotic bodies are phagocytosed by adjacent cells (c). Scale bar: 10  $\mu$ m (a), 4  $\mu$ m (b, c).

A



B

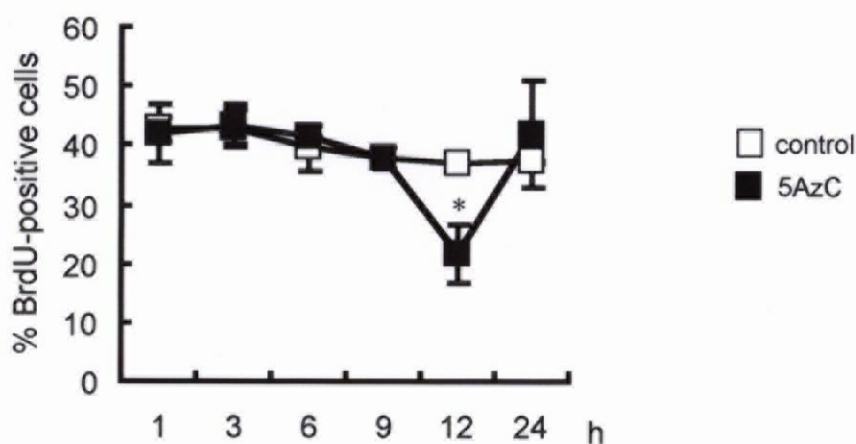


Fig. 1-3. Changes of BrdU-positive cells at S-phase in the telencephalic wall of 5AzC-treated and control fetuses. 5AzC was injected into dams at E13, and the fetuses were collected at 1, 3, 6, 9, 12, and 24 h after treatment. BrdU were injected at 1 h before sacrifice. A: Immunohistochemistry for BrdU. a: control at 12 h, b:1 h, c: 3 h, d: 6 h, e: 9 h, f: 12 h, g: 24 h after 5AzC-treatment. Scale bar: 50  $\mu$ m. B: Changes in the percentage of BrdU-positive cells in the telencephalic wall of 5AzC-treated (closed square) and control fetuses (open square). Each value represents the mean  $\pm$  SD of 2 dams. \*:  $p < 0.05$ ; significantly different from the control group (Student's *t*-test).

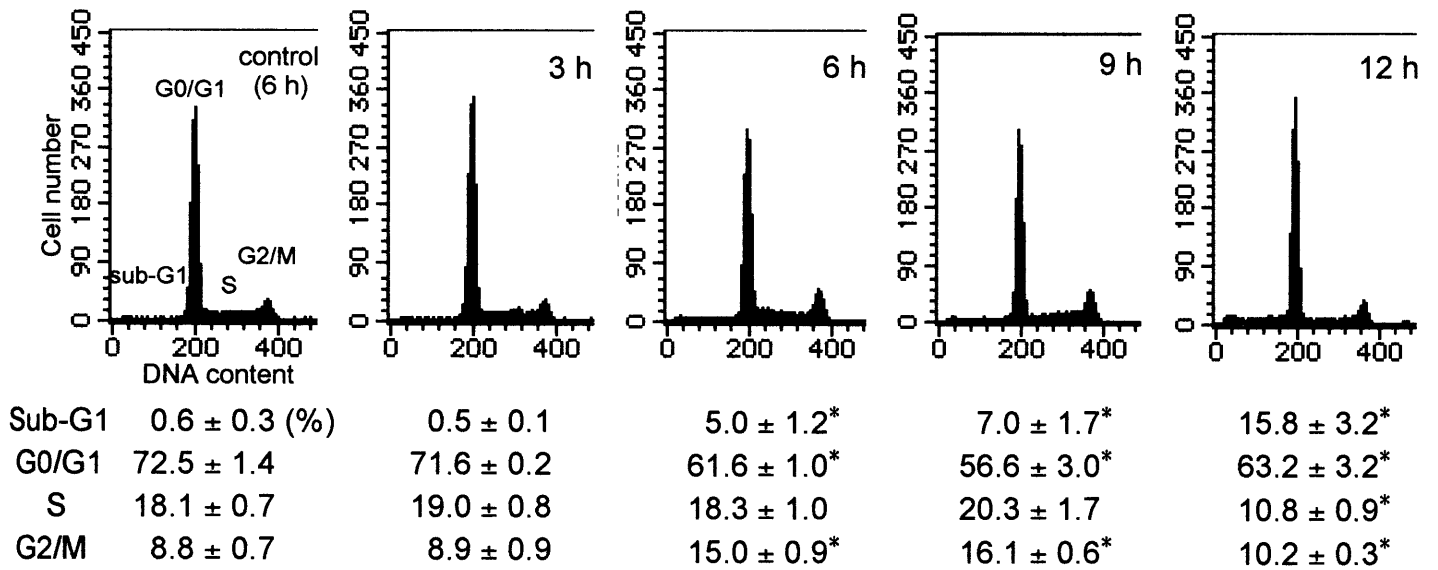


Fig. 1-4. Cell cycle analysis of telencephalic cells in the rat fetus (X axis: PI intensity (DNA content), Y axis: cell number). Percentages for each cell cycle phase are presented as the mean ± SD of 3 dams. The treatment of 5AzC increased the number of G2/M cells from 6 to 9 h, and apoptotic cells in the sub-G1 area from 6 to 12 h. \*:  $p < 0.05$ ; significantly different from the control (6 h) (Student's *t*-test).

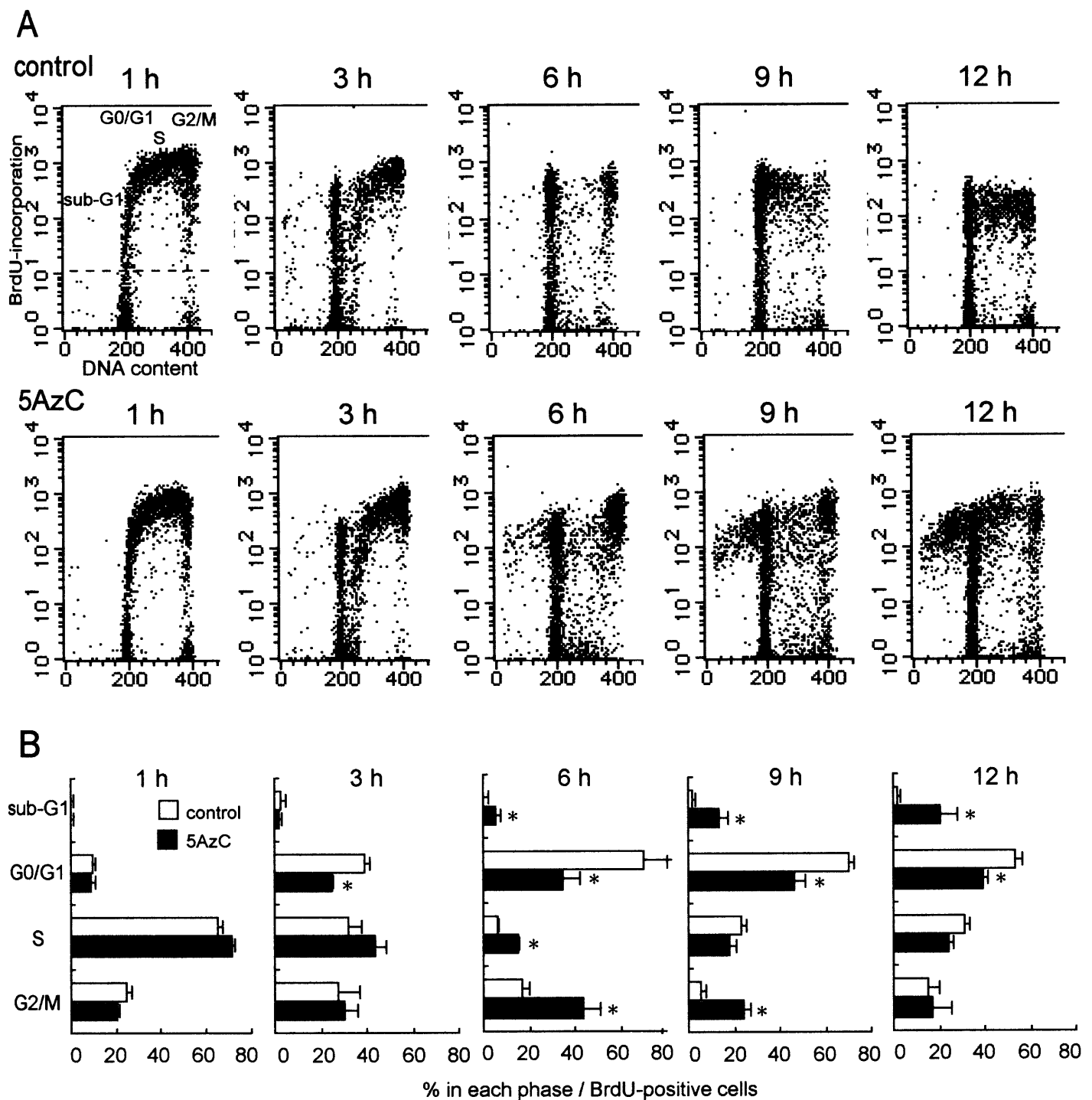


Fig. 1-5. Transition of BrdU-incorporated telencephalic cells of rat fetus in the cell cycle. A: Detection of BrdU-incorporated cells in the cell cycle using flow cytometry (X axis: PI intensity (DNA content), Y axis: FITC intensity (BrdU-incorporation)). The cells with FITC-intensity above the dotted line are BrdU-positive cells. B: Distribution of BrdU-positive cells in the cell cycle (white bar: control group, gray bar: 5AzC-treated group). Percentages for each cell cycle phase are presented as the mean  $\pm$  SD of 2 dams. \*:  $p < 0.05$ ; significantly different from the control group (Student's  $t$ -test). By 5AzC-treatment, BrdU-positive cells were accumulated in G2/M phase from 6 to 9 h, and then they transited to G0/G1 or sub-G1 area (apoptosis).

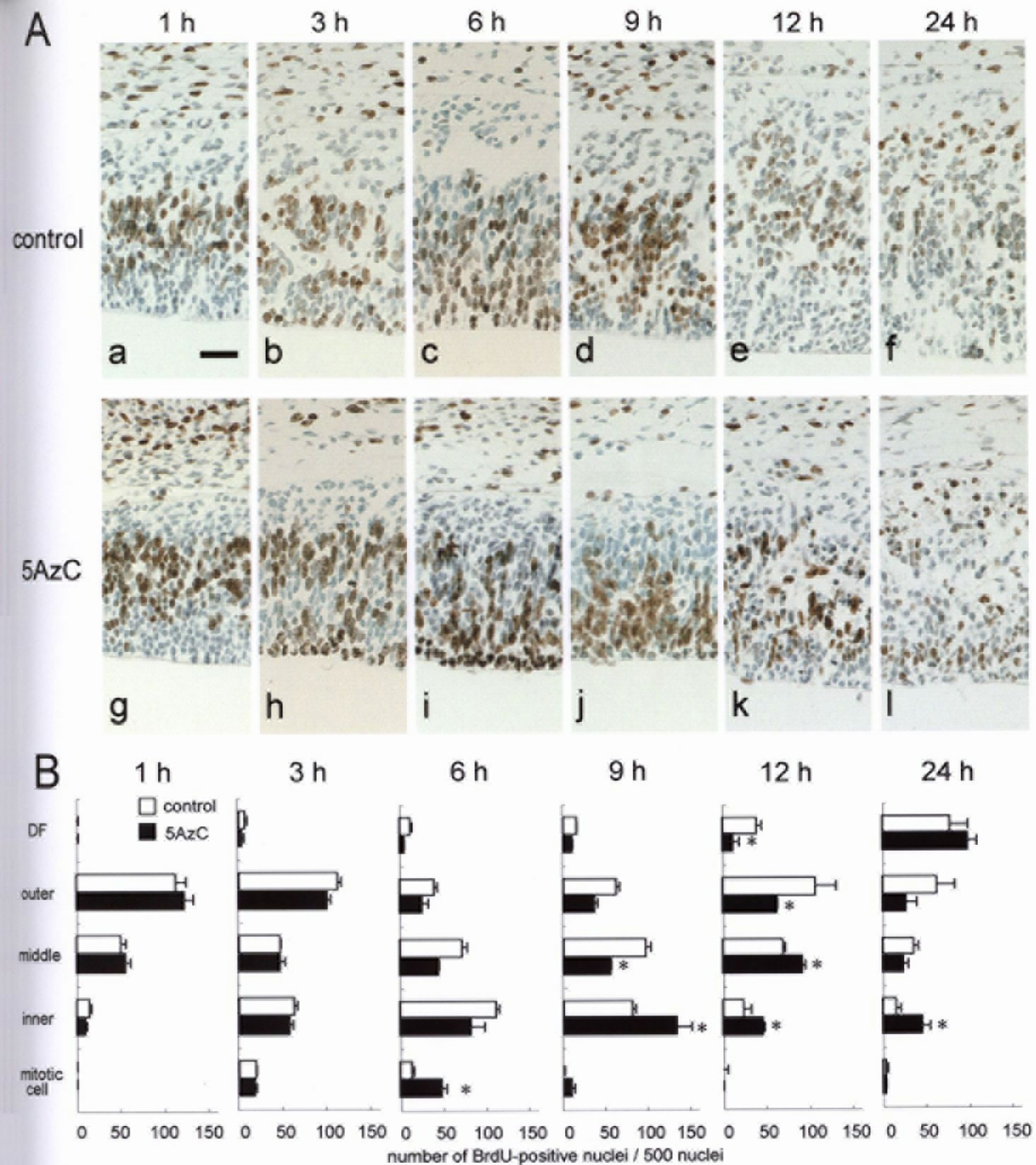
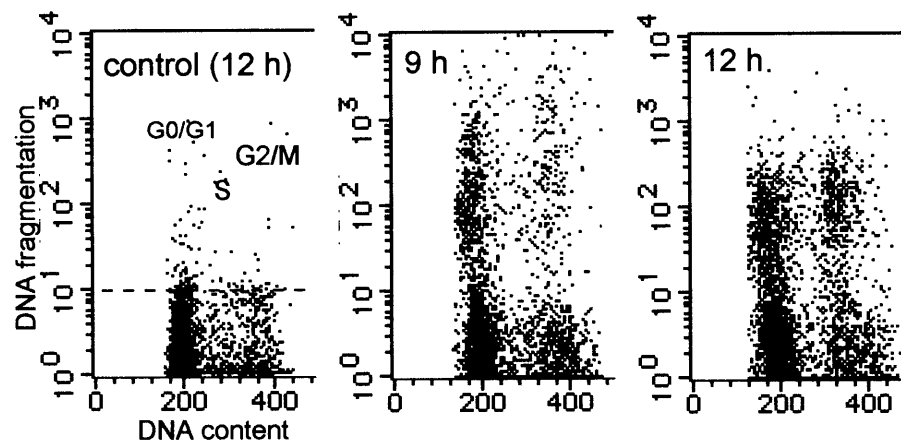


Fig. 1-6. Migration of BrdU-positive nuclei of neural progenitor cells in the telencephalic wall of 5 AzC-treated and control fetuses. BrdU alone was injected as controls, and 5AzC and BrdU were injected into dams at the same time at E13. **A**: Migration of BrdU-positive nuclei was detected immunohistochemically. Sections of control (a-f) and 5AzC-treated (g-l) fetuses were stained with anti-BrdU at 1 h (a, g), 3 h (b, h), 6 h (c, i), 9 h (d, j), 12 h (e, k), and 24 h (f, l) after BrdU treatment. For evaluating the migration of BrdU-positive nuclei, the telencephalic wall were divided into 5 areas (DF, outer, middle, inner, mitotic cells; Fig. I-2). Scale bar: 50  $\mu$ m. **B**: The number of BrdU-positive nuclei / 500 nuclei in each area of the telencephalic wall was counted. White bar: control, black bar: 5 AzC-treated group. Each value represents the mean  $\pm$  SD of 2 dams. \*:  $p < 0.05$ ; significantly different from the control group.



| Apoptotic cell | 1.8 ± 1.4 (%) | 10.5 ± 3.6 | 19.5 ± 2.1 |
|----------------|---------------|------------|------------|
| G0/G1          | 68.7 ± 5.4    | 65.0 ± 5.8 | 56.6 ± 3.7 |
| S              | 18.4 ± 4.5    | 9.2 ± 1.5  | 9.6 ± 1.3  |
| G2/M           | 12.9 ± 1.1    | 25.8 ± 4.9 | 33.8 ± 4.9 |

Fig. 1-7. Apoptotic cells and their DNA contents in 5AzC-treated rat fetal telencephalon (X axis: PI intensity (DNA content), Y axis: FITC intensity (DNA fragmentation)). The cells with FITC-intensity above the dotted line are BrdU-labeled apoptotic cells. Percentages of apoptotic cells and their cell cycle distribution are presented as the mean ± SD of 3 dams. 5AzC-induced apoptosis mainly occurred in G1, while also in G2/M and S phase.

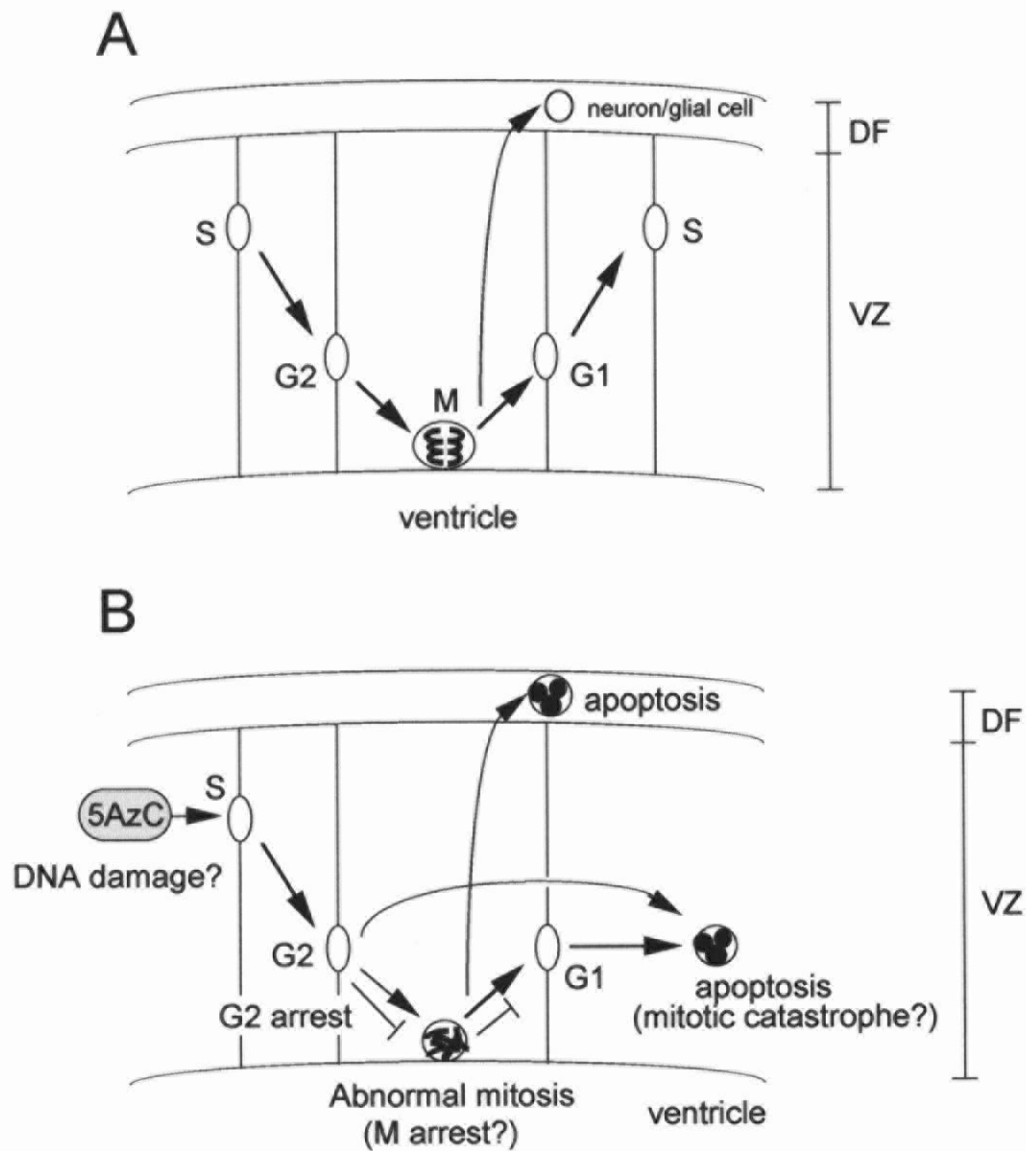


Fig. 1-8. Mechanism of 5AzC-induced toxicity in the developing fetal brain. A: Interkinetic nuclear migration of neural progenitor cells (see also Fig. I-2). Neural progenitor cells proliferate with their nuclei migrating up and down in the VZ. The positions of nuclei are correlated with the cell cycle phases. B: The schema of the mechanisms of 5AzC-induced cell cycle alteration and apoptosis. 5AzC would be incorporated into DNA in S phase and cause DNA damage. Damaged neural progenitor cells enter M phase with abnormal morphologies along the ventricle. G2 arrest also occurs with delay in inward-migration. Then, the cells are divided into daughter cells, but undergo apoptosis in G1 phase. G2 phase cells also die by apoptosis. Postmitotic cells undergo apoptosis in later stage when they migrate to the DF.